Effects of hyperonic many-body force on B_Λ values of hypernuclei

M. Isaka[1], Y. Yamamoto[2], and Th.A. Rijken[3,2]
[1] *Research Center for Nuclear Physics (RCNP), Osaka University, Ibaraki, Osaka, 567-0047, Japan*
[2] *Nishina Center for Accelerator-Based Science, Institute for Physical and Chemical Research (RIKEN), Wako, Saitama, 351-0198, Japan*
[3] *IMAPP, Radboud University, 6500 GL Nijmegen, The Netherlands*

(Dated: March 10, 2017)

The stiff equation of state (EoS) giving the neutron-star mass of $2M_\odot$ suggests the existence of strongly repulsive many-body effect (MBE) not only in nucleon channels but also in hyperonic ones. As a specific model for MBE, the repulsive multi-pomeron exchange potential (MPP) is added to the two-body interaction together with the phenomenological three-body attraction. For various versions of the Nijmegen interaction models, the MBE parts are determined so as to reproduce the observed data of B_Λ. The mass dependence of B_Λ values is shown to be reproduced well by adding MBE with the strong MPP repulsion assuring the stiff EoS of hyperon-mixed neutron-star matter, when P-state components of the adopted interaction model lead to almost vanishing contributions. The nuclear matter ΛN G-matrix interactions are derived and used in Λ hypernuclei on the basis of the averaged-density approximation (ADA). The B_Λ values of hypernuclei with $9 \leq A \leq 59$ are analyzed in the framework of Antisymmetrized Molecular Dynamics with use of the two types of ΛN G-matrix interactions including strong and weak MPP repulsions. The calculated values of B_Λ reproduce the experimental data finely within a few hundred keV. The values of B_Λ in p-states also can be reproduced well, when ADA is modified to be suitable also to weakly-bound Λ states.

PACS numbers: Valid PACS appear here

arXiv:1703.03117v1 [nucl-th] 9 Mar 2017

I. INTRODUCTION

Λ binding energies B_Λ are basic quantities in Λ hypernuclei. In 1950's the values of B_Λ were extracted from Λ hypernuclei with mass $A < 16$ observed in emulsion. After 1980's, medium and heavy Λ hypernuclei have been produced by counter experiments such as (π^+, K^+) reactions. Recently accurate data of B_Λ values in ground and excited states of hypernuclei have been obtained by γ-ray observations and $(e, e'K^+)$ reactions. On the other hand, theoretical baryon-baryon interaction models have been developed [1–7], where ΛN-ΣN coupling terms have been included in order to reproduce values of Λ single particle potentials U_Λ values in nuclear matter more or less realistically. Because hyperon(Y)-nucleon(N) scattering data are extremely limited, there remain remarkable ambiguities in YN interaction models: Values of U_Λ for various interaction models are substantially different from each other.

The YN interactions are related intimately to the recent topic in neutron-stars. The large observed masses of $2M_\odot$ [8, 9] give a severe condition for the stiffness of equation of state (EoS) of neutron-star matter. The stiff EoS giving the maximum mass of $2M_\odot$ can be derived from the existence of strong three-nucleon repulsion (TNR) in the high-density region. However, the hyperon (Y) mixing in neutron-star matter brings about the remarkable softening of the EoS, which cancels the TNR effect for the maximum mass [10–12]. This problem is known as the "Hyperon puzzle". It is considered that this puzzle can be solved if strong repulsions exist not only in NNN cannels but also in YNN and YYN channels [12].

Recently, there have been reported the trials to extract the ΛNN repulsions from the systematic data of B_Λ [13, 14]. In Refs.[13, 15], the multi-pomeron exchange potential (MPP) was added to the two-body baryon-baryon interaction V_{BB} together with the phenomenological three-body attraction (TBA). Then, the parameters included in MPP and TBA were determined so as to reproduce the angular distribution of ^{16}O+^{16}O scattering at $E/A = 70$ MeV and the nuclear saturation property, where the MPP contributions were decisive to reproduce the experimental angular distribution and brought about the stiff EoS enough to give maximum masses over $2M_\odot$. V_{BB} gives the potentials in NN and YN channels, and MPP is universal in all baryon channels. The TBA parts in YN channels are determined so as to reproduce hypernuclear data reasonably. On the basis of this (V_{BB}+MPP+TBA) model, it was shown that the EoS was still stiff enough to reproduce neutron stars with $2M_\odot$ in spite of substantial softening by hyperon mixing.

The aim of this work is to investigate the ΛN sectors of the V_{BB}+MPP+TBA model, especially the many-body effects (MBE) given by MPP+TBA parts, through structure calculations of Λ hypernuclei within the framework of the antisymmetrized molecular dynamics for hypernuclei (HyperAMD). When we determine the MPP+TBA part so as to reproduce the experimental values of B_Λ, it is evident that this part is dependent on the interaction model for V_{BB}. In other words, it is indispensable that reliable interaction models should be used for V_{BB} in order to investigate MBE. We start from the Nijmegen interaction models for V_{BB}, being reliable enough to extract MBE in spite of remained ambiguity for reproducing values of B_Λ.

In Refs.[14, 16], the strengths of ΛNN forces were determined by the fitting procedure to the data of B_Λ. Their ΛNN repulsion in the best fitting case seems to be

abnormally strong. The reason seems to be because they start from the two-body ΛN interaction with no ΛN-ΣN term, giving an overbinding value of U_Λ.

In our case, the ΛN-ΣN coupling terms are included in the Nijmegen models so that their strengths are determined to reproduce physical observables through channel-coupling effects to ΛN-ΛN diagonal channels. Then, there remains a rather small room for MBE around normal-density region, where the MPP and TBA contributions are cancelled substantially with each other. In our previous work [17], referred to I, the experimental values of B_Λ have been reproduced systematically by the HyperAMD calculations using a special Nijmegen model having only a very small room for MBE. In Ref. [17], even in this case it was demonstrated that the small MBE works to improve the fitting of B_Λ values to experimental data. In this work, we show that they appear more clearly in the case of using the updated versions of Nijmegen extended-soft core (ESC) models.

This paper is organized as follows. In the next section, the various versions of the Nijmegen models and MBE (MPP+TBA) are explained, and the ΛN G-matrix calculations are performed. Different features of interaction models are discussed by showing U_Λ values in nuclear matter. In Sec. III, the detailed analysis for Λ hypernuclei with $9 \leq A \leq 59$ are performed on the basis of HyperAMD with use of G-matrix interactions including MBE. It is discussed what feature of the two-body interaction allows the existence of strong repulsion suggested by the stiff EoS of neutron stars. Section V summarizes this paper.

II. U_Λ IN NUCLEAR MATTER

A. Nijmegen interaction models

The meson-theoretical models for YN interactions have been developed continuously by the Nijmegen group. In the earlier stage, they developed the hard-core models [18] (NHC-D and -F) and the soft-core model (NSC89) [1]. After that, the trial started to take into account the G-matrix results in the modeling of YN interactions. As the first outcome of this approach, the NSC97 models [2] were proposed, where the six versions a$\sim$f were designed so as to be of different strengths of the ΛN spin-spin parts. Then, the observed splitting energies of spin-doublet states in Λ hypernuclei suggested that the spin-spin strengths of NSC97e and NSC07f were in a reasonable region. Epoch-making development of the Nijmegen models was accomplished by the ESC models, in which two-meson and meson-pair exchanges are taken into account explicitly. In the one-boson exchange (OBE) models these effects are implicitly and roughly described by exchanges of 'effective mesons'. After some trial versions, there appeared the specific versions ESC04a/b/c/d [3], features of which were very different from those of the OBE models especially in $S = -2$ channels. However, there remain some serious problems in NSC97 and ESC04 models. The first is that the derived values of Λ spin-orbit splitting energies are too large in comparison with the experimental values. The second is that the derived Σ-nucleus potentials U_Σ are attractive, whereas the experimental values are indicated to be repulsive. Furthermore, the ΞN interactions seem to be unreliable: The U_Ξ values derived from the NSC97 (ESC04a/b) models are strongly (weakly) repulsive. Those for ESC04c/d are attractive, but their partial-wave contributions seem to be rather problematic. These problems have been further investigated in ESC08a/b/c [4] where the treatments for axial-vector and pair terms are improved, and the effects of the quark Pauli-forbidden states in the repulsive-core representation are taken into account. However, in these models the ΞN cross sections are too large. At present the possibility is investigated to replace in U_Ξ part of the two-body attraction by a three-body force contribution. This trial to improve the ΞN part does not affect the NN and $YN(S = -1)$ parts.

Here, in order to investigate sizes of MBE needed for different interaction models, we pick up ESC08a/b/c, ESC04a and NSC97e/f among the various the Nijmgen models. In Ref. [17], we used ESC08c in an early stage of parameter fitting: This version denoted as ESC08c(2012) [19], and the recent version as ESC08c(2014) [20–22]. Hereafter, ESC08c(2012) and ESC08c(2014) are denoted simply as ESC12 and ESC14, respectively. These two versions of ESC08c are used in this work mainly.Very recently, there is given the latest version ESC08c(2016) [23], ESC16, though it is not used in this work. The reason why we pick up ESC04a (NSC97e/f) among ESC04a/b/c/d (NSC97a/b/c/d/f) is because ESC04b/c/d give more attractive values of U_Λ than ESC04a, and NSC97a/b/c are with unreasonable spin-spin parts, not giving binding of ${}^{3}_{\Lambda}$H.

One of the ideas to avoid remarkable softening of neutron-star EoS by hyperon mixing is to assume that the strong three-body repulsions work universally for YNN, YYN YYY as well as for NNN [12]. As a model of universal repulsions among three and four baryons, we introduce the multi-pomeron exchange potential (MPP). Additionally to MPP, the three-baryon attraction (TBA) is assumed phenomenologically. MPP and TBA in nucleon channels are determined so as to reproduce the experimental angular distributions of ^{16}O+^{16}O elastic scattering (E/A=70 MeV) and the nuclear saturation property. In hyperonic channels, they should be taken consistently with hypernuclear data: For each interaction model V_{BB}, MPP and TBA parts are adjusted so as to reproduce experimental data of B_Λ as well as possible.

The specific form of MPP is given as the N-body local potential by pomeron exchange $W^{(N)}(\mathbf{x}_1, ..., \mathbf{x}_N)$ [13, 15] and the effective two-body potential in a baryonic medium is obtained by integrating over the coordinates

$\mathbf{x}_3, ..., \mathbf{x}_N$;

$$V^{(N)}_{MPP}(\mathbf{x}_1, \mathbf{x}_2)$$
$$= \rho^{N-2} \int d^3x_3 ... \int d^3x_N \; W^{(N)}(\mathbf{x}_1, \mathbf{x}_2, ..., \mathbf{x}_N)$$
$$= g_P^{(N)} g_P^N \frac{\rho^{N-2}}{\mathcal{M}^{3N-4}} \cdot \left(\frac{m_P}{\sqrt{2\pi}}\right)^3 \exp\left(-\frac{1}{2} m_P^2 r_{12}^2\right) . \quad (1)$$

We assume that the dominant mechanism is triple and quartic pomeron exchange. The values of the two-body pomeron strength g_P and the pomeron mass m_P are taken from the adopted ESC model. A scale mass $\mathcal{M}$ is taken as a proton mass. TBA is assumed as a density-dependent two-body interaction

$$V_{TBA}(r; \rho)$$
$$= V_0 \; \exp(-(r/2.0)^2) \, \rho \, \exp(-\eta\rho) \, (1 + P_r)/2 \; , \quad (2)$$

P_r being a space-exchange operator. There are given the three sets with different strengths of MPP [13, 15]. We consider the set MPa as a guidance in this work, where the parameters are taken as $g_P^{(3)} = 2.34$, $g_P^{(4)} = 30.0$, $V_0 = -32.8$ and $\eta = 3.5$. Then, the most important is whether or not such a strongly repulsion given by these values of $g_P^{(3)}$ and $g_P^{(4)}$ is allowable in reproducing the mass dependence of B_Λ values.

B. G-matrix interaction

We start from the channel-coupled G-matrix equation for the baryon pair B_1B_2 in nuclear matter [24], where $B_1B_2 = \Lambda N$ and ΣN:

$$G_{cc_0} = v_{cc_0} + \sum_{c'} v_{cc'} \frac{Q_{y'}}{\omega - \epsilon_{B_1'} - \epsilon_{B_2'} + \Delta_{yy'}} G_{c'c_0} \; , \quad (3)$$

where c denotes a YN relative state (y, T, L, S, J) with $y = (B_1B_2)$. S and T are spin and isospin quantum numbers, respectively. Orbital and total angular momenta are denoted by L and J, respectively, with $\mathbf{J} = \mathbf{L} + \mathbf{S}$. Then, a two-particle state is represented as ${}^{2S+1}L_J$. In Eq. (3), ω gives the starting energy in the channel c_0. $\Delta_{yy'} = M_{B_1} + M_{B_2} - M_{B_1'} - M_{B_2'}$ denotes the mass difference between two baryon channels. The Pauli operator Q_y acts on intermediate nucleon states in a channel $y = (B_1B_2) = (\Lambda N$ and $\Sigma N)$. The continuous (CON) choice is adopted for intermediate single particle potentials in the G-matrix equation.

The G-matrix equation (3) is represented in the coordinate space, whose solutions give rise to G-matrix elements. The hyperon single particle (s.p.) energy ϵ_Y in nuclear matter is given by

$$\epsilon_Y(k_Y) = \frac{\hbar^2 k_Y^2}{2M_Y} + U_Y(k_Y) \; , \quad (4)$$

TABLE I: Λ potential energies U_Λ [MeV] at normal density for adopted interaction models. $U_\Lambda(S)$ and $U_\Lambda(P)$ are S- and P-state contributions, respectively, in unit of MeV.

	U_Λ	$U_\Lambda(S)$	$U_\Lambda(P)$
ESC08a	-40.6	-39.5	$+0.5$
ESC08b	-39.4	-37.0	-0.6
ESC14	-40.8	-39.6	$+0.4$
ESC12	-40.0	-40.0	$+1.5$
ESC04a	-43.2	-38.4	-3.7
NSC97e	-37.7	-40.4	$+4.0$
NSC97f	-34.8	-39.1	$+5.6$

where k_Y is the hyperon momentum. The potential energy U_Y is obtained self-consistently in terms of the G-matrix as

$$U_Y(k_Y) =$$
$$\sum_{|\mathbf{k}_N|} \langle \mathbf{k}_Y \mathbf{k}_N \mid G_{YN}(\omega = \epsilon_Y + \epsilon_N) \mid \mathbf{k}_Y \mathbf{k}_N \rangle \quad (5)$$

In Table I, we show the potential energies U_Λ of a zero-momentum Λ at normal density ρ_0 (k_F=1.35 fm^{-1}). Their S- and P-state contributions are given by $U_\Lambda(S)$ and $U_\Lambda(P)$, respectively. They are calculated for adopted Nijmegen models. It is noted that the U_Λ values for ESC08a/b, ESC14 and ESC12 are rather similar to each other, and those for NSC97e/f (ESC04a) are less (more) attractive due to strongly repulsive (attractive) P-state contributions. As is given in [23], we have $U_\Lambda = -39.6$ MeV, $U_\Lambda(S) = -38.8$ MeV and $U_\Lambda(P) = +0.7$ MeV for ESC16. It's S-(P-) contribution is slightly less attaractive (more repulsive) than those for ESC14.

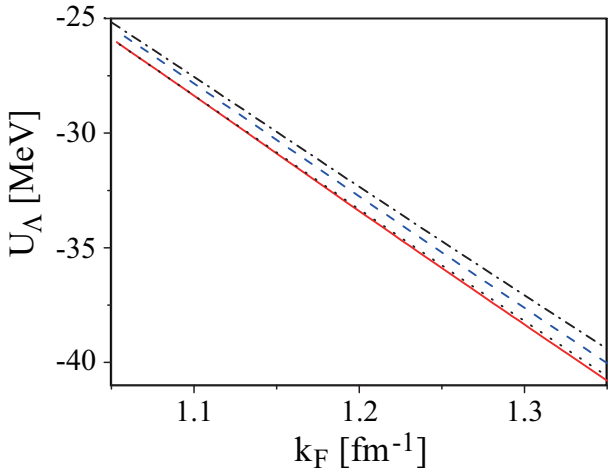

FIG. 1: (Color online) U_Λ as a function of k_F. Solid, dashed, dotted and dot-dashed curves are for ESC14, ESC12, ESC08a and ESC08b, respectively.

In Fig.1, Fig.2 and Fig.3, respectively, U_Λ, $U_\Lambda(S)$ and $U_\Lambda(P)$ are drawn as a function of k_F in the cases of ESC08 models. Here, solid, dashed, dotted and

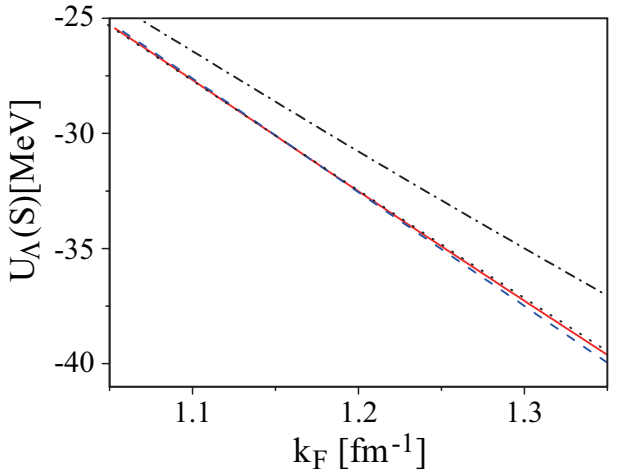

FIG. 2: (Color online) S-state contributions to U_Λ as a function of k_F. Also see the caption of Fig.1.

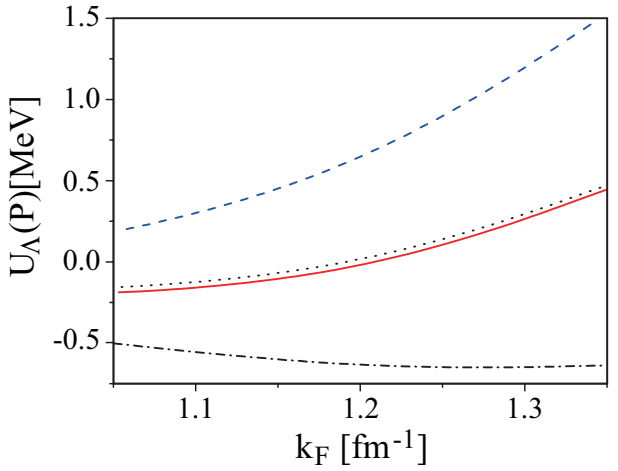

FIG. 3: (Color online) P-state contributions to U_Λ as a function of k_F. Also see the caption of Fig.1.

dot-dashed curves are for ESC14, ESC12, ESC08a and ESC08b. It is found that the curves for ESC14 and ESC08a are very similar to each other, and the main difference among those for ESC14, ESC08a, ESC12 and ESC08b is in the P-state contributions. In Fig.3, the important point is that the P-state contributions for ESC14 and ESC08a are almost vanishing in the region of $k_F = 1.1 \sim 1.2$ fm^{-1}. This feature appears also in case of ESC16, and means that the P-state contributions are small for B_Λ values in light hypernuclei. On the other hand, there appears the repulsive contribution substantially in the case of ESC12. As discussed later, the sizes of P-state contributions are related to a room to take MBE effects into account.

For structure calculations of Λ hypernuclei, we derive k_F-dependent effective local potentials $\mathcal{G}(k_F; r)$, simulating ΛN G-matrices. They are parameterized in a three-range Gaussian form:

$$\mathcal{G}(k_F, r) = \sum_{i=1}^{3} (a_i + b_i k_F + c_i k_F^2) \exp\left(-r^2/\beta_i^2\right) . \quad (6)$$

The parameters (a_i, b_i, c_i) are determined so as to simulate the calculated G-matrix for each $^{2S+1}L_J$ state. The procedures to fit the parameters are given in Ref. [24]. The parameters for $\mathcal{G}(k_F, r)$ for ESC14 are given in Table II . It should be noted that $\mathcal{G}(k_F, r)$ are adjusted so as to reproduce exactly the values of U_Λ in nuclear matter. Contributions from $V_{MPP}^{(3)}$, $V_{MPP}^{(4)}$ and $V_{TBA}(r; \rho)$ are taken into account by modifying the second-range parts of $\mathcal{G}(k_F, r)$ by $\Delta\mathcal{G}(k_F, r) = (a + bk_F + ck_F^2) \exp -(r/\beta_2)^2$.

Here, B_Λ values in finite systems are calculated by using Λ-nucleus potentials in which ΛN G-matrix $\mathcal{G}(k_F, r)$ interactions are folded into density distributions [24]. Then, in order to treat k_F values included in G-matrix interactions, we use the averaged-density approximation (ADA), given as,

$$k_F = \left(\frac{3\pi^2\langle\rho\rangle}{2}\right)^{1/3}, \langle\rho\rangle = \int d^3r \rho_N(\mathbf{r})\rho_\Lambda(\mathbf{r}), \quad (7)$$

where $\rho_N(\mathbf{r})$ and $\rho_\Lambda(\mathbf{r})$ represent the densities of the nucleons and Λ particle, respectively. In the next section, as well as in Ref. [17], the HyperAMD is used for structure calculations of Λ hypernuclei based on ADA. For spherical-core systems, it is confirmed that the present

TABLE II: Parameters in $\mathcal{G}(k_F; r) = \sum_{i=1}^{3}(a_i + b_i k_F + c_i k_F^2) \exp -(r/\beta_i)^2$ for ESC14. a_i [MeV], b_i [MeV·fm], c_i [MeV·fm^2], and β_i [fm] are given for each i.

	β_i	0.50	0.90	2.00
^1E	a_i	−3434.	396.0	−1.708
	b_i	6937.	−1057.	0.0
	c_i	−2635.	415.9	0.0
^3E	a_i	−1933.	195.4	−1.295
	b_i	4698.	−732.8	0.0
	c_i	−1974.	330.1	0.0
^1O	a_i	206.1	67.89	−.8292
	b_i	−30.52	34.11	0.0
	c_i	16.23	2.471	0.0
^3O	a_i	2327.	−254.1	−.9959
	b_i	−2361.	202.6	0.0
	c_i	854.3	−43.71	0.0

TABLE III: Parameters a [MeV], b [MeV·fm], and c [MeV·fm^2] in $\Delta\mathcal{G}(k_F; r) = (a + bk_F + ck_F^2) \exp -(r/\beta_2)^2$ with $\beta_2 = 0.9$ fm in the case of $g_P^{(3)} = 2.34$, $g_P^{(4)} = 30.0$ and $V_0 = -21.0$.

	^1E	^3E	^1O	^3O
a	20.71	19.16	26.31	24.95
b	−51.74	−49.31	−73.58	−71.92
c	28.84	27.30	64.01	66.73

TABLE IV: ΔB_Λ [MeV] defined as $\Delta B_\Lambda = B_\Lambda(^{89}_{\Lambda}\mathrm{Y}) - B_\Lambda(^{16}_{\Lambda}\mathrm{O})$. The experimental values of ΔB_Λ and $B_\Lambda(^{89}_{\Lambda}\mathrm{Y})$ are 10.7 MeV and 23.7 MeV, respectively. Values in parentheses are calculated without MPP+TBA parts.

	$g_P^{(3)}$	$g_P^{(4)}$	V_0	ΔB_Λ	$B_\Lambda(^{89}_{\Lambda}\mathrm{Y})$
ESC08a	2.34	30.0	−21.0	10.9 (13.3)	24.2 (26.6)
ESC08b	2.34	30.0	−29.0	10.9 (12.3)	24.1 (24.2)
ESC14	2.34	30.0	−21.0	10.8 (13.2)	24.0 (26.5)
ESC12	0.39	0.0	−5.0	10.6 (10.8)	23.9 (23.7)
NSC97e	0.39	0.0	−8.0	10.4 (10.1)	24.0 (22.8)
NSC97f	0.0	0.0	−13.0	10.3 (8.7)	23.8 (20.2)

TABLE V: ΔB_Λ and $B_\Lambda(^{89}_{\Lambda}\mathrm{Y})$ for ESC14 and ESC12. Values in (a) are calculated with MPP+TBA, and values in (b) and (c) are calculated only with MPP and TBA, respectively.

	ΔB_Λ	$B_\Lambda(^{89}_{\Lambda}\mathrm{Y})$
ESC14		
(a) MPP+TBA	10.8	24.0
(b) MPP	7.9	17.9
(c) TBA	16.1	33.4
ESC12		
(a) MPP+TBA	10.6	23.9
(b) MPP	10.0	22.3
(c) TBA	11.4	25.2
exp	10.7	23.7

G-matrix folding model and the HyperAMD give rise to similar results with each other.

Now, MPP and TBA parts are determined so that the experimental values of B_Λ are reproduced by calculations with the G-matrix folding model and the HyperAMD. In the cases of ESC08a/b and ESC14, the experimental data can be reproduced well by varying only V_0 in TBA for values of $g_P^{(3)} = 2.34$ and $g_P^{(4)} = 30.0$ in the MPa set, being fixed to assure the stiffness of the neutron-star matter. In Table III, The parameters in $\Delta\mathcal{G}(k_F, r)$ are given in the case of $g_P^{(3)} = 2.34$, $g_P^{(4)} = 30.0$ and $V_0 = -21.0$, being adequate for ESC14. The parameters in $\Delta\mathcal{G}(k_F, r)$ for ESC12 are given in Ref. [17].

In the cases of ESC12 and NSC97e/f, it is needed to take far smaller values of $g_P^{(3)}$ and $g_P^{(4)}$ for good fitting. In the case of ESC04a, we obtain no reasonable set of $g_P^{(3)}$, $g_P^{(4)}$ and V_0, which indicates that the ESC04 models are inadequate to find reasonable MBE. Table IV gives determined values of $g_P^{(3)}$, $g_P^{(4)}$ and V_0 and calculated values of $\Delta B_\Lambda = B_\Lambda(^{89}_{\Lambda}\mathrm{Y}) - B_\Lambda(^{16}_{\Lambda}\mathrm{O})$ and $B_\Lambda(^{89}_{\Lambda}\mathrm{Y})$ by the G-matrix folding model for each interaction model. Here, the values of ΔB_Λ are used to demonstrate roughly the mass dependence of B_Λ values. The values in parentheses are obtained without the MPP+TBA part $\Delta\mathcal{G}(k_F, r)$. It should be noted that only in the case of ESC12 the calculated values reproduces well the experimental values of ΔB_Λ and $B_\Lambda(^{89}_{\Lambda}\mathrm{Y})$ without contributions of $\Delta\mathcal{G}(k_F, r)$.

As found in Table I, the order of P-state repulsions $U_\Lambda(P)$ is NSC97f>NSC97e>ESC12. This order corresponds to that of the attractions V_0 in Table IV, where the stronger repulsion is needed to be cancelled by the stronger attraction.

Table V gives calculated values of ΔB_Λ and $B_\Lambda(^{89}_{\Lambda}\mathrm{Y})$ for ESC14 and ESC12. Values in (a) are calculated with MPP+TBA, being the same ones in the Table IV. Values in (b) and (c) are calculated only with MPP and TBA, respectively. In the case of ESC14, values of ΔB_Λ and $B_\Lambda(^{89}_{\Lambda}\mathrm{Y})$ including only MPP (TBA) are far smaller (larger) than those including MPP+TBA. Thus, we find that the reasonable values for MPP+TBA are owing to substantial canceling between MPP and TBA contributions. On the other hand, both contributions of MPP and TBA are small.

From Figs.1, 2, and 3, some features can be found: One is that the results for ESC14 and ESC08a are very similar to each other. Their even-state parts give overbinding values of B_Λ, where the odd-state parts are weak. Then, MBE plays a role to lift them up to experimental values. As shown in ref.[23], this feature appears also in the case of ESC16. On the other hand, in the case of ESC12 the even-state parts are more attractive than those of ESC14 and ESC08a, and the strongly repulsive odd-state parts contribute to reproduce the B_Λ values, and there remains only a small room for MBE to improve fitting. Then, it is very important that the odd-state contributions are relatively smaller than the even-state ones in low-density region. In the case of ESC12 the mass dependence of B_Λ values, being estimated roughly by ΔB_Λ, can be reproduced well owing to this feature of odd-state contributions. In the left (right) side of Fig.4, the U_Λ curves are given for ESC14 (ESC12), where solid (dashed) curves are with (without) the MPP+TBA contributions. It is found that the contribution from the MPP+TBA part in the ESC14 case is much larger than that in the ESC12 case. The k_F dependence of U_Λ is (not) changed significantly by MBE in the former (latter) case. Dot-dashed (dotted) curves in these figures show U_Λ values only with MPP (TBA). In the case of ESC14, the solid curve with MPP+TBA turns out to be obtained by substantial canceling between MPP and TBA contributions.

As found in Fig.1, the U_Λ curve for ESC08b is similar to that for ESC12. However, the $U_\Lambda(S)$ values for ESC08b are considerably less attractive than that for ESC12, and $U_\Lambda(P)$ values for ESC08b (ESC12) are attractive (strongly repulsive). Due to this feature of ESC08b, the B_Λ values are of rather underbinding, and the experimental values are reproduced by adding the large attractive contributions from the MPP+TBA parts. In the cases of NSC97e/f, the odd-state contributions are more repulsive than those for ESC12 and there is no room of strong-MPP contribution.

Thus, it should be noted that a room for MBE is dependent sensitively on the odd-state part in the ΛN interaction, which has not yet been established experimentally

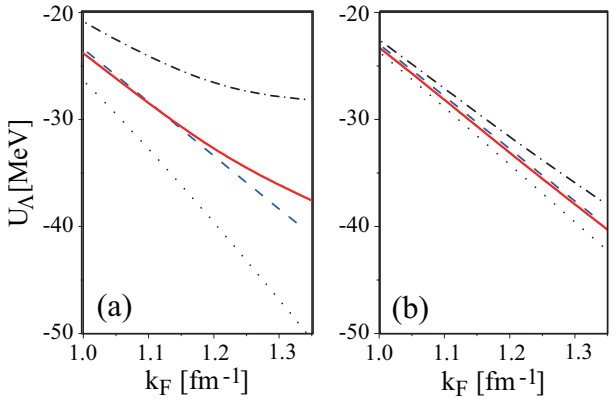

FIG. 4: (Color online) (a) U_Λ curves with ESC14. Solid (dashed) curve shows U_Λ with (without) the MPP+TBA contributions. Dot-dashed (dotted) curve shows U_Λ only with MPP (TBA). (b) Same as (a), but for ESC12.

in the present stage.

III. ANALYSIS OF B_Λ VALUES BASED ON HYPERAMD

In this Section, we discuss how the difference in U_Λ of the ΛN two-body interactions appears and affects the MBE in the systematics of B_Λ. As for the V_{BB}, we focus on ESC14 and ESC12 with MBE, because ESC08a/b are very similar to ESC14 as demonstrated in the previous section, and ESC12 is considerably different from ESC08a/b and ESC14 in odd states. In this section, the calculations are performed with use of ESC14 and ESC12. In our previous work [17], based on ESC12, it was found that B_Λ is sensitive to the structure of core nuclei, in particular core deformations. Furthermore, sophisticated treatment of k_F related to core structure is also essential for quantitative discussion of B_Λ. In the present work, we perform structure calculations based on ESC14 within the framework of HyperAMD based on ADA from ${}^{9}_{\Lambda}$Li up to ${}^{59}_{\Lambda}$Fe, being compared with the results in Ref. [17]. The G-matrix interaction for ESC16 in Ref.[23] is considered to give the result similar to that for ESC14.

A. Framework of HyperAMD

The Hamiltonian used in this study is

$$H = T_N + T_\Lambda - T_g + V_{NN} + V_C + V_{\Lambda N}, \qquad (8)$$

where T_N, T_Λ, and T_g are the kinetic energies of the nucleons, Λ particle, and center-of-mass motion, respectively. V_{NN} and V_C are the effective nucleon-nucleon (NN) and Coulomb interactions, respectively. The Coulomb interaction V_C is approximated by the sum of seven Gaussians. As for the ΛN interaction $V_{\Lambda N}$, we use the G-matrix interaction discussed above.

In this study we use the Gogny D1S force [43, 44] as the effective NN interaction V_{NN}. In our previous work [17], it was found that structure of the core nuclei affects the values of B_Λ. This fact tells us that proper description of core structure is indispensable to extract information of ΛN interaction from the B_Λ values in a model approach. Therefore, we need to use an appropriate effective NN interaction in the HyperAMD calculation, which gives better agreement with the observed data in wide mass regions. The Gogny D1S force is one of such effective interactions. It is found that the AMD calculation with Gogny D1S force successfully describes core deformations and gives reasonable binding energies of the core nuclei within a few percent of deviation from the observed data.

The variational wave function of a single Λ hypernucleus is described by the parity-projected wave function, $\Psi^\pm = \hat{P}^\pm\{\mathcal{A}\{\varphi_1, \ldots, \varphi_A\} \otimes \varphi_\Lambda\}$, where

$$\varphi_i \propto e^{-\sum_\sigma \nu_\sigma \left(r_\sigma - Z_{i\sigma}\right)^2} \otimes (u_i\chi_\uparrow + v_i\chi_\downarrow) \otimes (p \text{ or } n), \quad (9)$$

$$\varphi_\Lambda \propto \sum_{m=1}^{M} c_m e^{-\sum_\sigma \nu_\sigma \left(r_\sigma - z_{m\sigma}\right)^2} \otimes (a_m\chi_\uparrow + b_m\chi_\downarrow). \quad (10)$$

Here the single-particle wave packet of a nucleon φ_i is described by a single Gaussian, while that of Λ, φ_Λ, is represented by a superposition of Gaussian wave packets. The variational parameters $\boldsymbol{Z}_i$, $\boldsymbol{z}_m$, ν_σ, u_i, v_i, a_m, b_m, and c_m are determined to minimize the total energy under the constraint on the nuclear quadrupole deformation (β, γ), and the optimized wave function $\Psi^\pm(\beta, \gamma)$ is obtained for each given (β, γ).

After the variation, we project out the eigenstate of the total angular momentum J for each set of (β, γ),

$$\Psi^{J\pm}_{MK}(\beta, \gamma) = \frac{2J+1}{8\pi^2} \int d\Omega D^{J*}_{MK}(\Omega) R(\Omega) \Psi^\pm(\beta, \gamma). \qquad (11)$$

The integrals over the three Euler angles Ω are performed numerically. Then the wave functions with different values of K and (β, γ) are superposed (generator coordinate method; GCM):

$$\Psi^{J\pm}_n = \sum_p \sum_{K=-J}^{J} c_{nK} \Psi^{J\pm}_{MK}(\beta_p, \gamma_p), \qquad (12)$$

where n represents quantum numbers other than total angular momentum and parity. The coefficients c_{npK} are determined by solving the Griffin-Hill-Wheeler equation. After the GCM calculation, we obtain both the ground and excited states of hypernuclei as shown in Fig. 5, where the present calculation nicely reproduces the observed spectra of ${}^{13}_{\Lambda}$C.

In order to see the importance of describing the core deformation, we also perform the GCM calculation by us-

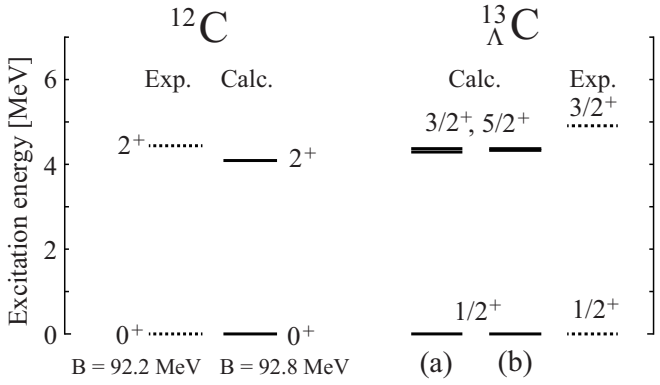

FIG. 5: Excitation spectra of ^{12}C and $^{13}_{\Lambda}$C with (a) ESC12 + MBE and (b) ESC14 + MBE. Observed energy spectrum of $^{13}_{\Lambda}$C by the γ ray spectroscopy experiments [47] is also displayed.

ing the intrinsic wave function with $\beta = 0.0$ only, namely,

$$\Psi^{J\pm}_n = \sum_{K=-J}^{J} c_{npK} \Psi^{J\pm}_{MK}(\beta = 0.0), \tag{13}$$

and compare it with the usual GCM calculations given by Eq. (12), which was done in Ref. [17].

The B_Λ is calculated as the energy difference between the ground states of a hypernucleus ($^{A+1}_{\Lambda}Z$) and the core nucleus (^{A}Z) as $B_\Lambda = E(^{A}Z; j^\pm) - E(^{A+1}_{\Lambda}Z; J^\pm)$, where $E(^{A}Z; j^\pm)$ and $E(^{A+1}_{\Lambda}Z; J^\pm)$ are calculated by GCM.

We also calculate the squared overlap between the $\Psi^{J\pm}_{MK}(\beta,\gamma)$ and GCM wave function $\Psi^{J\pm}_n$,

$$O^{J\pm}_{MKn}(\beta,\gamma) = |\langle \Psi^{J\pm}_{MK}(\beta,\gamma) | \Psi^{J\pm}_n \rangle|^2, \tag{14}$$

which is called the GCM overlap. $O^{J\pm}_{MKn}(\beta,\gamma)$ shows the contribution of $\Psi^{J\pm}_{MK}(\beta,\gamma)$ to each state $J^\pm$, which is useful to estimate the deformation of each state. In this study, we regard (β,γ) corresponding to the maximum value of the GCM overlap as the nuclear deformation of each state.

B. Impact of MBE on mass dependence of B_Λ

On the basis of ESC14 and ESC12, we discuss the effects of MBE on B_Λ values. In Table VI, the values of B_Λ calculated with HyperAMD are summarized together with the experimental values of B_Λ ($B^{\rm exp}_\Lambda$). It is noted that the values of $B^{\rm exp}_\Lambda$ with dagger are shifted deeper by 0.54 MeV from those reported in Refs. [25, 26, 28, 39, 40], concerning the systematic difference of $B^{\rm exp}_\Lambda$ between the emulsion and (π^+, K^+) (or (K^-, π^-)) experiments, which was pointed out by Ref. [42]. In Table VI, we also show the χ^2 values calculated by using the experimental and theoretical values of B_Λ for the hypernuclei with asterisk to see the agreement of each other. As discussed in Ref. [17], in cases of $^{9}_{\Lambda}$Be, $^{15}_{\Lambda}$N and $^{28}_{\Lambda}$Si, the calculated values of B_Λ deviate considerably from the experimental values by the inherent reason for each system. Therefore, we exclude these hypernuclei from the evaluation of the χ^2 values.

Before the discussions on MBE, let us see the calculated values of B_Λ without MBE (V_{BB} only in Table VI). Comparing ESC14 with ESC12, it is seen that the B_Λ for ESC12 without MBE are rather close to the experimental data. This is clearly seen in the χ^2 values without MBE, i.e. the χ^2 value for ESC12 ($\chi^2 = 38.7$) is much smaller than that for ESC14 ($\chi^2 = 87.7$). However, this value for ESC12 is not extremely small, which indicates that there still exists a room to improve the fitting by adding MBE. In the case of ESC14, the calculated values of B_Λ are deviated much from the observations. In particular, in the medium-heavy hypernuclei, the B_Λ values for ESC14 become larger than those with ESC12, and overestimate the $B^{\rm exp}_\Lambda$ considerably. For example, in $^{51}_{\Lambda}$V, the calculated value of B_Λ for ESC14 is 23.5 MeV, whereas $B_\Lambda = 20.4$ MeV for ESC12 (*cf.* $B^{\rm exp}_\Lambda = 20.51 \pm 0.13$ MeV [40]). This is mainly due to the difference of the P-state interactions of ESC14 and ESC12. In Fig. 3 the P-state contribution for ESC14 is found to be far smaller than that of ESC12, while the S-state contributions for ESC14 and ESC12 are similar to each other. Then, the difference of the P-state contributions for ESC14 and ESC12 appears more clearly in B_Λ values of heavier hypernuclei than in those of lighter ones, because P-state contributions are relatively small in light systems.

Next, let us discuss the MBE on the mass dependence of B_Λ. From the analysis in Sec. II, we use different parameter sets of MBE combined with ESC14 and ESC12, as shown in Table IV. In the case of ESC14, the MPP part of the MPa set ($g^{(3)}_P = 2.34$ and $g^{(4)}_P = 30.0$) is used, which gives the stiff EoS of the neutron star matter. In ESC12 with MBE, the parameters $g^{(3)}_P$, $g^{(4)}_P$ and V_0 are determined so as to reproduce the $B^{\rm exp}_\Lambda$ in $^{16}_{\Lambda}$O without considering the stiffness of the EoS, and show nice agreement with $B^{\rm exp}_\Lambda$ in the wide mass regions [17]. As a result, the strength of the MBE part combined with ESC12 is much weaker than that with ESC14. Hereafter, ESC14 (ESC12) combined with MBE is denoted as ESC14+MBE (ESC12+MBE).

In Table VI, the values of B_Λ calculated with ESC14+MBE are also summarized together with those by using ESC12+MBE taken from Ref. [17]. It is found that the B_Λ values for ESC14+MBE, as well as ESC12+MBE, reproduce the observed data within about 200 keV in the $9 \le A \le 59$ regions except for $^{9}_{\Lambda}$Be, $^{15}_{\Lambda}$N, and $^{28}_{\Lambda}$Si. It is clearly seen that the χ^2 values are reduced by including MBE ($\chi^2 = 4.63$ for ESC14+MBE and $\chi^2 = 3.61$ for ESC12+MBE), which means that the agreement of B_Λ is improved significantly by including MBE. Here, it has no meaning to discuss the difference in the two small χ^2 values, because we did not search these values exactly as minimum values for variation of the parameters included in MBE.

TABLE VI: Comparison of $-B_\Lambda$ [MeV] with including MBE by MPP + TBA based on ESC12 and ESC14. Values of B_Λ by using ESC12 with/without MBE are taken from Ref. I [17]. k_F [fm^{-1}] value calculated under ADA are also listed together with $\langle\rho\rangle$ [fm^{-3}] defined by Eq. (7). Observed values $B_\Lambda^{\rm exp}$ are taken from Refs. [25–28, 37–42]. Values of $B_\Lambda^{\rm exp}$ with dagger are explained in text. χ^2 values calculated with B_Λ and $B_\Lambda^{\rm exp}$ for the hypernuclei with $(*)$ are also listed. The ground state spin-parity J^π calculated and observed are also shown.

			Based on ESC12 [17]				Based on ESC14					
			V_{BB} only		w/ MBE		V_{BB} only		w/ MBE		Expt.	
	$\langle\rho\rangle$	k_F	J^π	$-B_\Lambda$	J^π	$-B_\Lambda$	J^π	$-B_\Lambda$	J^π	$-B_\Lambda$	J^π	$-B_\Lambda^{\rm exp}$
${}^{9}_{\Lambda}$Li$(*)$	0.072	1.02	$5/2^+$	−7.9	$5/2^+$	−8.1	$5/2^+$	−7.6	$5/2^+$	−8.1	–	-8.50 ± 0.12[37]
${}^{9}_{\Lambda}$Be	0.060	0.96	$1/2^+$	−7.9	$1/2^+$	−8.1	$1/2^+$	−7.7	$1/2^+$	−8.1	$1/2^+$	-6.71 ± 0.04[38]
${}^{9}_{\Lambda}$B$(*)$	0.072	1.02	$5/2^+$	−8.0	$5/2^+$	−8.2	$5/2^+$	−7.7	$5/2^+$	−8.2	–	-8.29 ± 0.18[37]
${}^{10}_{\Lambda}$Be$(*)$	0.077	1.04	2^-	−8.7	2^-	−9.0	2^-	−8.6	2^-	−9.0	–	-9.11 ± 0.22[27], -8.55 ± 0.18[42]
${}^{10}_{\Lambda}$B$(*)$	0.075	1.04	2^-	−8.9	2^-	−9.2	2^-	−8.7	2^-	−9.1	1^-[29, 30]	-8.89 ± 0.12[38]
${}^{11}_{\Lambda}$B$(*)$	0.081	1.05	$7/2^+$	−9.8	$7/2^+$	−10.1	$7/2^+$	−9.7	$7/2^+$	−10.0	$5/2^+$[31]	-10.24 ± 0.05[38]
${}^{12}_{\Lambda}$B$(*)$	0.083	1.07	2^-	−11.0	2^-	−11.3	2^-	−11.0	2^-	−11.3	1^-[32–34]	-11.37 ± 0.06[38], -11.38 ± 0.02[41]
${}^{12}_{\Lambda}$C$(*)$	0.086	1.08	2^-	−10.7	2^-	−11.0	2^-	−10.8	2^-	−11.0	1^-[35]	-10.76 ± 0.19[37]
${}^{13}_{\Lambda}$C$(*)$	0.090	1.10	$1/2^+$	−11.3	$1/2^+$	−11.6	$1/2^+$	−11.5	$1/2^+$	−11.7	$1/2^+$	-11.69 ± 0.19[27]
${}^{14}_{\Lambda}$C$(*)$	0.093	1.11	0^-	−12.4	0^-	−12.5	0^-	−12.4	0^-	−12.5	–	-12.17 ± 0.33[37]
${}^{15}_{\Lambda}$N	0.098	1.13	$1/2^+$	−12.6	$1/2^+$	−12.9	$1/2^+$	−12.9	$1/2^+$	−12.9	$3/2^+$[29]	-13.59 ± 0.15[38]
${}^{16}_{\Lambda}$O$(*)$	0.105	1.16	0^-	−12.7	0^-	−13.0	1^-	−13.3	1^-	−13.0	0^-[36]	-12.96 ± 0.05[28]†
${}^{19}_{\Lambda}$O	0.110	1.18	$1/2^+$	−14.0	$1/2^+$	−14.3	$1/2^+$	−14.8	$1/2^+$	−14.3	–	–
${}^{21}_{\Lambda}$Ne	0.106	1.20	$1/2^+$	−15.1	$1/2^+$	−15.4	$1/2^+$	−15.8	$1/2^+$	−15.5	–	–
${}^{25}_{\Lambda}$Mg	0.116	1.23	$1/2^+$	−15.8	$1/2^+$	−16.1	$1/2^+$	−17.0	$1/2^+$	−16.1	–	–
${}^{27}_{\Lambda}$Mg	0.125	1.23	$1/2^+$	−16.1	$1/2^+$	−16.3	$1/2^+$	−17.5	$1/2^+$	−16.2	–	–
${}^{28}_{\Lambda}$Si	0.125	1.23	2^+	−16.4	2^+	−16.6	2^+	−17.8	2^+	−16.6	–	-17.1 ± 0.02[25, 48]†
${}^{32}_{\Lambda}$S$(*)$	0.130	1.24	0^+	−17.4	0^+	−17.6	1^+	−19.4	0^+	−17.6	–	-18.0 ± 0.5[26]†
${}^{40}_{\Lambda}$K	0.136	1.26	1^+	−19.2	1^+	−19.4	1^+	−21.5	1^+	−19.4	–	–
${}^{40}_{\Lambda}$Ca$(*)$	0.136	1.26	1^+	−19.2	1^+	−19.4	1^+	−21.3	1^+	−19.3	–	-19.24 ± 1.1[39]†
${}^{41}_{\Lambda}$Ca	0.136	1.26	$1/2^+$	−19.4	$1/2^+$	−19.6	$1/2^+$	−21.5	$1/2^+$	−19.5	–	–
${}^{48}_{\Lambda}$K	0.141	1.27	1^+	−20.1	1^+	−20.2	1^+	−22.6	1^+	−20.2	–	–
${}^{51}_{\Lambda}$V$(*)$	0.151	1.31	$11/2^+$	−20.4	$11/2^+$	−20.4	$11/2^+$	−23.5	$11/2^+$	−20.3	–	-20.51 ± 0.13[40]†
${}^{59}_{\Lambda}$Fe	0.142	1.28	$1/2^+$	−21.3	$1/2^+$	−21.4	$1/2^+$	−24.6	$1/2^+$	−21.7	–	–
χ^2 for $(*)$				38.7		3.61		87.7		4.63		

For the fine agreements of B_Λ, the MBE part plays an essential role, especially in ESC14+MBE, which is clearly seen in the comparison of B_Λ between ESC14 and ESC14+MBE in Table VI. In the hypernuclei with $A \geq 16$, where the ESC14 causes overbinding of B_Λ, the MBE essentially acts as a repulsive force and shifts the B_Λ to be close to the observed values. For example, in ${}^{51}_{\Lambda}$V, B_Λ is shifted from 23.5 MeV to 20.3 MeV by adding MBE. In the light hypernuclei, the MBE gives attraction. In ESC14+MBE, the MPP repulsion acts strongly at high density or large k_F, which gives the stiff EoS of the neutron-star matter, and becomes weaker as k_F decreases, while TBA remains at small k_F regions. Thus, the MBE gives attraction in the light hypernuclei with smaller values of k_F.

In the case of ESC12, the MBE brings about the minor changes of B_Λ as seen in Table VI. This is because the MPP and TBA combined with ESC12 are much weaker than those with ESC14. It is noted that the weak MPP in ESC12+MBE is inconsistent with the stiff EoS suggested by the massive neutron star. It is also found that if the strong MPP included in ESC14+MBE is combined with ESC12, the derived values of B_Λ contradict the observed data. Therefore, based on ESC12, there is no choice of MBE to satisfy both the observed data of B_Λ and the stiff EoS of the neutron star matter. This indicates that the strong repulsion suggested by the massive neutron star imposes a stringent constraint on the ΛN two-body interaction models. From the results in Table VI, we conclude that the ESC14 is one of the ΛN interaction models which satisfies these conditions. As discussed in the previous section, ESC08a/b are similar to ESC14 on this point. P-state interactions in ESC14 and ESC08a/b are not strongly repulsive differently from ESC12, and do not play a role to reproduce the mass dependence of B_Λ values. Namely, there is a room for adding MBE with strong MPP repulsion owing to the weak P-state contribution.

In the light hypernuclei, as pointed out in Ref. [17], it is also important to describe properly the core structure, especially deformations of the core nuclei, to reproduce B_Λ, because it can affect the B_Λ through the k_F dependence of the interaction. In order to see the effects by core deformations, we compare the B_Λ values calculated

by performing the full-basis GCM (see Eq. (12)) and spherical GCM (see Eq. (13)) calculations. In Fig. 6, it is seen that B_Λ calculated by the spherical GCM are shallower than those in the full-basis GCM calculation and deviated from $B_\Lambda^{\rm exp}$, which is clearly seen in the χ^2 values. In the spherical GCM calculation with ESC12+MBE, the χ^2 is 171, whereas $\chi^2 = 4.63$ in the full-basis GCM calculation. This is because spherical states make k_F larger through the increase of $\langle\rho\rangle$ in Eq. (7). The difference of B_Λ in Fig. 6 is quite similar to the results with ESC12 in Ref. [17].

In Tab. VI, the spin and parity J^π are also listed for the ground states of the hypernuclei together with those known by the experiments. In case of the core nuclei having non-zero spin in the ground states, such as ^{11}C and ^{10}B, we naturally obtain the spin doublets in the corresponding hypernuclei, generated by coupling a Λ particle with spin 1/2 to the ground states of the core nuclei. For example, in $^{12}_{\Lambda}$C, we obtain the $(1^-, 2^-)$ doublet corresponding to the ^{11}C ground-state $(3/2^-)$. In Tab. VI, it is seen that the calculated ground-state is $J^\pi = 2^-$, which is different from the observation ($J = 1^-$). Similarly, in $^{11}_{\Lambda}$B, we obtain the $J^\pi = 7/2^+$ state as the ground state among the $(5/2^+, 7/2^+)$ doublet, whereas the $5/2^+$ state is the lowest in the experiment. This discrepancy is attributed to the property of the ΛN spin-dependent interaction, which was discussed for the series of the ESC08 interaction models in Ref. [24]. In $^{12}_{\Lambda}$C, from the observed ground-state 1^-, one can notice that the spin-singlet ΛN interaction is slightly more attractive than the spin-triplet interaction. In the present calculation, it is considered that the spin-triplet part of the ΛN interaction is slightly strong. Thus, the detailed properties of the spin dependence of the ΛN interaction could affect the ordering of the ground-state doublet partners, though it has little influence on the B_Λ curve.

Finally, we also comment on the energy change of the nuclear part by the addition of a Λ particle, namely the rearrangement energy ΔE_N. Since B_Λ is defined by the energy difference of the ground states between a hypernucleus and the core nucleus, it contains not only the Λ single particle energy but also the energy changes of the core part, in which the former corresponds to the sum of the expectation values of T_Λ and $V_{\Lambda N}$ and the latter is the ΔE_N. Therefore, the rearrangement energy ΔE_N is defined as,

$$\Delta E_N = \frac{\langle\Psi_n^{J\pm}|H_N|\Psi_n^{J\pm}\rangle}{\langle\Psi_n^{J\pm}|\Psi_n^{J\pm}\rangle} - E(^AZ; j^\pi), \qquad (15)$$

$$H_N = T_N + V_{NN} + V_C, \qquad (16)$$

where $\Psi_n^{J\pm}$ is the GCM wave function defined by Eq. (12). In Table VII, we summarize ΔE_N together with the ground-state energies of the core nuclei for the several hypernuclei with the different mass regions. It is found that the rearrangements energies are in order of a few hundred keV, which are quite smaller compared with B_Λ. Furthermore, it is also seen that ΔE_N is reduced as mass number increases. This is because adding a Λ particle cannot change the core nuclei significantly, if the core nucleus is large enough.

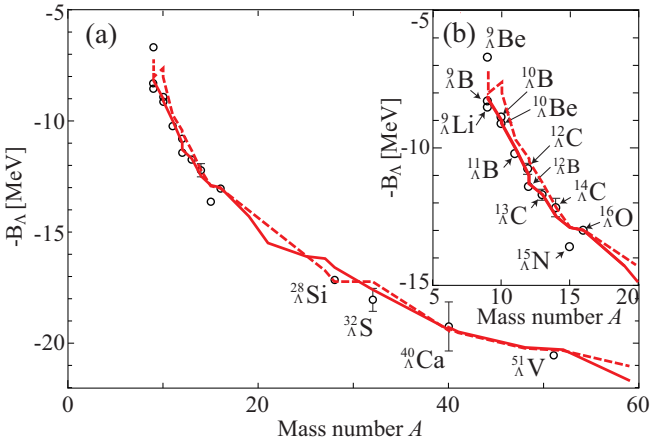

FIG. 6: (Color online) (a) Comparison of B_Λ between full-basis GCM (solid) and spherical GCM (dashed) calculations. Open circles show observed data with mass numbers from $A = 9$ up to $A = 51$, which are taken from Refs. [25–28, 37–41]. $B_\Lambda^{\rm exp}$ measured by (π^+, K^+) and (K^-, π^-) reactions are shifted by 0.54 MeV as explained in text. (b) Same as (a), but magnified in the $5 \le A \le 20$ region.

TABLE VII: Rearrangement energies ΔE_N [MeV], defined by Eq. (15), calculated for the ground states J^π of the hypernuclei with different mass regions by using ESC14+MBE. Calculated ($E_{\rm core}$) and observed ($E_{\rm core}^{\rm exp}$) energies of the ground states $J^\pi_{\rm core}$in the core nuclei are also listed in MeV.

	J^π	ΔE_N	$J^\pi_{\rm core}$	$E_{\rm core}$	$E_{\rm core}^{\rm exp}$[45]
$^{9}_{\Lambda}$B	$5/2^+$	0.24	2^+	-41.5	-37.7
$^{13}_{\Lambda}$C	$1/2^+$	0.16	0^+	-92.8	-92.2
$^{28}_{\Lambda}$Si	2^+	0.14	$5/2^+$	-219.7	-219.4
$^{41}_{\Lambda}$Ca	$1/2^+$	0.03	0^+	-341.7	-342.0
$^{48}_{\Lambda}$K	1^+	0.03	$1/2^+$	-400.2	-389.0

C. B_Λ in p-states

Let us focus on excited p-states of hypernuclei, in which the Λ particle in p-orbit is bound to the ground state of the core nucleus. In general, since the Λ particle in $p_{1/2}$ and $p_{3/2}$ orbits can couple to the core nuclei, several p states appear. In this paper, we focus on the lowest p state in excitation energy for each hypernucleus. In Sec. III B, the HyperAMD calculation nicely reproduces the observed data of B_Λ in the ground states of the hypernuclei using ESC12+MBE and ESC14+MBE by taking into account their structures, where the ADA treatment works well to obtain appropriate values of k_F from the wave functions of the hypernuclei. In this section, we discuss the B_Λ values in the p-states for the light ($^{12}_{\Lambda}$B, $^{13}_{\Lambda}$C,

TABLE VIII: Calculated (experimental) binding energy B_Λ ($B_\Lambda^{\rm exp}$) and excitation energy E_x ($E_x^{\rm exp}$) for the p-states J^π in MeV together with ρ [fm^{-3}] and k_F [fm^{-1}] calculated by Eqs. (7). $B_\Lambda^{\rm exp}$ with $\dagger\dagger$($E_x^{\rm exp}$ with $\dagger\dagger\dagger$) are calculated by using $E_x^{\rm exp}$ ($B_\Lambda^{\rm exp}$) of the p-states and the $B_\Lambda^{\rm exp}$ values shown in Table VI.

			ESC12+MBE			ESC14+MBE			Exp.	
	$\langle\rho\rangle$	k_F	J^π	$-B_\Lambda$	E_x	J^π	$-B_\Lambda$	E_x	$-B_\Lambda^{\rm exp}$	$E_x^{\rm exp}$
$^{12}_{\Lambda}$B	0.069	0.92	3^+	-2.4	8.8	3^+	-2.4	8.9	-1.289 ± 0.048 [41]	10.24 ± 0.05 [41]
$^{13}_{\Lambda}$C	0.067	1.00	$1/2^-$	-2.1	9.5	$1/2^-$	-2.4	9.3	$-0.9^{\dagger\dagger}$	10.830 ± 0.087 [46, 47]
									$-1.96^{\dagger\dagger}$	9.73 ± 0.14 [28]
$^{16}_{\Lambda}$O	0.068	1.00	3^+	-3.9	9.1	3^+	-4.0	9.0	$-2.39^{\dagger\dagger}$	10.57 ± 0.06 [28]
$^{28}_{\Lambda}$Si	0.101	1.14	3^-	-8.0	8.6	3^-	-8.4	8.2	-7.5 ± 0.2 [48]†	$9.6^{\dagger\dagger\dagger}$
$^{51}_{\Lambda}$V	0.124	1.22	$11/2^-$	-12.7	7.7	$11/2^-$	-13.1	7.2	-12.44 ± 0.17 [40]†	$8.07^{\dagger\dagger\dagger}$

TABLE IX: Same as Table VIII but with a correction of k_F as $k'_F = (1+\alpha)k_F$.

		ESC12+MBE				ESC14+MBE				Exp.	
	$\langle\rho\rangle$	k'_F	J^π	$-B_\Lambda$	E_x	k'_F	J^π	$-B_\Lambda$	E_x	$-B_\Lambda^{\rm exp}$	$E_x^{\rm exp}$
		$\alpha = 0.070$				$\alpha = 0.070$					
$^{12}_{\Lambda}$B	0.069	0.98	3^+	-0.7	10.6	0.98	3^+	-0.8	10.5	-1.289 ± 0.048 [41]	10.24 ± 0.05 [41]
$^{13}_{\Lambda}$C	0.067	1.07	$1/2^-$	-0.9	10.8	1.07	$1/2^-$	-1.0	10.7	$-0.9^{\dagger\dagger}$	10.830 ± 0.087 [46, 47]
										$-1.96^{\dagger\dagger\dagger}$	9.73 ± 0.14 [28]
$^{16}_{\Lambda}$O	0.068	1.07	0^+	-2.2	10.8	1.07	2^+	-2.6	10.4	$-2.39^{\dagger\dagger}$	10.57 ± 0.06 [28]
		$\alpha = 0.020$				$\alpha = 0.025$					
$^{28}_{\Lambda}$Si	0.101	1.17	3^-	-7.4	9.2	1.17	3^-	-7.5	9.1	-7.5 ± 0.2 [48]†	$9.6^{\dagger\dagger\dagger}$
		$\alpha = 0.010$				$\alpha = 0.015$					
$^{51}_{\Lambda}$V	0.124	1.24	$11/2^-$	-12.3	8.1	1.24	$11/2^-$	-12.5	7.8	-12.44 ± 0.17[40]†	$8.07^{\dagger\dagger\dagger}$

and $^{16}_{\Lambda}$O) and medium-heavy ($^{28}_{\Lambda}$Si and $^{51}_{\Lambda}$V) hypernuclei. In these hypernuclei, the p-states were observed in various experiments. The (π^+, K^+) reaction experiments show the peak structure corresponding to the p-states in $^{13}_{\Lambda}$C [28], $^{16}_{\Lambda}$O [28], $^{28}_{\Lambda}$Si [48], and $^{51}_{\Lambda}$V [40]. In $^{13}_{\Lambda}$C, the excitation energy of the p-states was precisely measured by the γ-ray spectroscopy experiment [46, 47]. Recently, in $^{12}_{\Lambda}$B, the $(e, e'K^+)$ reaction experiment was performed at Thomas Jefferson National Accelerator Facility (JLab), which shows clear peaks regarded as the p-states with high resolution [41].

Table VIII shows the calculated values of B_Λ and the excitation energies E_x of p-states with ESC12+MBE and ESC14+MBE together with the observed values. The calculated values of B_Λ are found to be slightly overbound by $0.3 \sim 1.1$ MeV in comparison with the observed data. Now, let us try to modify the choice of k_F values in ADA so as to reproduce B_Λ correctly, considering that the ADA might be changed suitably for weak Λ bound states: We tune the k_F value in ADA as $k'_F = (1+\alpha)k_F$ by introducing a parameter α, which is taken adequately for each mass region. For the light systems with $B_\Lambda \sim$ a few MeV, we take $\alpha = 0.070$ so as to reproduce the experimental values of B_Λ in the p-state of $^{13}_{\Lambda}$C ($B_\Lambda^{\rm exp} = 0.9$ MeV). Here, the $B_\Lambda^{\rm exp}$ of $^{13}_{\Lambda}$C is obtained by subtracting the excitation energy $E_x^{\rm exp} = 10.830 \pm 0.087$ MeV measured by the γ-ray spectroscopy [46, 47] from the $B_\Lambda^{\rm exp}$ in the ground state shown in Table VI. The calculated values of B_Λ and E_x with $\alpha = 0.070$ are shown in Table IX. In the both cases with ESC12+MBE and ESC14+MBE, it is found that the $B_\Lambda^{\rm exp}$ and $E_x^{\rm exp}$ in $^{13}_{\Lambda}$C are reproduced using almost the same α. In Table IX, it is seen that the values of B_Λ and E_x calculated with $\alpha = 0.070$ are much closer to the experimental values than those without α in $^{12}_{\Lambda}$B and $^{16}_{\Lambda}$O.

In $^{28}_{\Lambda}$Si and $^{51}_{\Lambda}$V with stronger binding of Λ, it is found that smaller values of α give reasonable values of B_Λ and E_x. Again, we tune k_F so as to reproduce $B_\Lambda^{\rm exp}$ in the p-states of $^{28}_{\Lambda}$Si and determine α as $\alpha = 0.025$ ($\alpha = 0.020$) with ESC14+MBE (ESC12+MBE). In $^{51}_{\Lambda}$V, it is also found that the $B_\Lambda^{\rm exp}$ and $E_x^{\rm exp}$ in the p-states are reproduced with $\alpha = 0.015$ ($\alpha = 0.010$) using ESC14+MBE (ESC12+MBE). These values of α in $^{28}_{\Lambda}$Si and $^{51}_{\Lambda}$V are much smaller than that determined in $^{13}_{\Lambda}$C. Thus, larger values of α turn out to be needed, as Λ bindings become weaker. It is worthwhile to point out, here, that the energy spectrum of $^{89}_{\Lambda}$Y can be reproduced nicely without the α parameter for the present G-matrix interactions with use of the Λ-nucleus folding model [13].

The degree of the modification of ADA by the α parameter is dependent on the smallness of B_Λ. As shown in Table IX, the $B_\Lambda^{\rm exp}$ values are in order of 1 MeV in $^{12}_{\Lambda}$B and $^{13}_{\Lambda}$C hypernuclei, which are much smaller than those in their ground states and the p-states of the medium-heavy hypernuclei. Therefore, p-state Λ particles in light hypernuclei are rather weakly bound. Generally, in weakly

bound states, since the Λ particle distributes in broader region around the core nucleus, the k_F value evaluated by Eq.(7) under ADA could be smaller and then it makes the B_Λ values larger. The above result shows that it brings about some overbinding of Λ to use Eq.(7) naively for weakly-bound Λ states. Then, the α parameter plays a role to make k_F larger and correct the overdoing of increase of B_Λ by smaller k_F values. In heavier hypernuclei with increasing B_Λ, the above effect is less important, and thus α can be smaller. It is demonstrated in Table IX that there is a good correspondence between the decrease of B_Λ values and the increase of α values. Thus, the present calculation reproduces the $B_\Lambda^{\rm exp}$ in p-states based on ADA with only a minor correction of k_F. This shows the validity of the HyperAMD calculations with the G-matrix interactions for applying to not only the ground states but also p-states of Λ hypernuclei with large mass regions.

D. ${}^{40}_{\Lambda}$K and ${}^{48}_{\Lambda}$K hypernuclei

At JLab, it is planned to perform the $(e, e'K)$ reaction experiment by using ^{40}Ca and ^{48}Ca as the target, i.e. potassium hypernuclei (${}^{40}_{\Lambda}$K and ${}^{48}_{\Lambda}$K) are expected to be produced [49]. As seen in Fig. 6, B_Λ values were measured in several hypernuclei in this mass region. However, only a few observed data of B_Λ are available. Furthermore, some of them have large ambiguities. For example, in ${}^{40}_{\Lambda}$Ca, the B_Λ in the ground state has a large error (more than 1 MeV). Since absolute energies of hypernuclei can be measured with high resolution in the spectroscopy experiment at JLab, precise values of B_Λ will be available for not only in the ground states but also excited states in ${}^{40}_{\Lambda}$K and ${}^{48}_{\Lambda}$K. Therefore, it is expected that the validity of the present calculation could be confirmed by comparing with the JLab experiments in heavier hypernuclei with $40 \leq A < 50$.

Recently, in this mass region, the effect by the isospin dependence of ΛNN force is discussed [50]. By the auxiliary field diffusion Monte Carlo (AFDMC) calculation [49, 50], it is shown that if the isospin dependence exists, it affects the B_Λ values in neutron-rich Λ hypernuclei such as ${}^{48}_{\Lambda}$K due to the asymmetry of the proton and neutron numbers. In the present study, our many-body force is isospin-independent, which affects strongly on the mass dependence of B_Λ even in neutron-rich hypernuclei. On the other hand, in our ΛN G-matrix interactions, the charge-dependent components included in the ESC model are not taken into account. On the basis of our present modeling for the ΛN interaction, we predict the values of B_Λ in ${}^{40}_{\Lambda}$K and ${}^{48}_{\Lambda}$K in the ground and p-states.

In Table X, the calculated values of B_Λ in the ground states with ESC12 + MBE and ESC14 + MBE are presented, which are taken from Table VI, i.e. these values are calculated without modifying ADA. It is found that the B_Λ value in ${}^{48}_{\Lambda}$K is larger than that in ${}^{40}_{\Lambda}$K. As seen in Fig. 6, these values are consistent with the mass dependence of B_Λ. Therefore, the B_Λ obtained by the present calculation becomes larger as the mass number increases. In the calculation for the p-states of ${}^{40}_{\Lambda}$K and ${}^{48}_{\Lambda}$K, we introduce small parameter α as $k'_F = (1+\alpha)k_F$ in the ADA treatment in the same manner as in Sec. III C. From the results of ${}^{28}_{\Lambda}$Si and ${}^{51}_{\Lambda}$V, it is expected that the appropriate value of α is in between 0.015 and 0.025 (0.010 and 0.020) in the p-states of ${}^{40}_{\Lambda}$K and ${}^{48}_{\Lambda}$K with ESC14 + MBE (ESC12 + MBE). Therefore, we calculate the B_Λ in the p-states using these values of α. The resulting values of B_Λ in the p-states are also summarized in Table X. In the case of ESC14 + MBE, it is found that the ambiguity of B_Λ coming from the α parameter is only about 300 keV, and the B_Λ values are predicted to be 10.1 MeV $\leq B_\Lambda \leq$ 10.4 MeV and 11.3 MeV $\leq B_\Lambda \leq$ 11.6 MeV for ${}^{40}_{\Lambda}$K and ${}^{48}_{\Lambda}$K, respectively. These values are in between those in ${}^{28}_{\Lambda}$Si and ${}^{51}_{\Lambda}$V, and are increased depending on the mass number. We find the same trend of B_Λ with the ESC12 + MBE. These values of B_Λ are expected to be compared with the future experiments at JLab, which could give us useful information on properties of hyperonic many-body force.

IV. SUMMARY

Basic quantities in hypernuclei are Λ binding energies B_Λ which lead to a potential depth U_Λ in nuclear matter. In spite of the longstanding development of studies for ΛN interactions, values of U_Λ derived from various interaction models are substantially different from each other: There still remain ambiguities of models due to lack of (accurate) YN scattering data.

The stiff EoS giving the neutron-star mass of $2M_\odot$ suggests the existence of strongly repulsive many-body effect (MBE) in the high-density region. On the other hand, the hyperon mixing in neutron-star matter brings about the remarkable softening of the EoS. In order to solve this "Hyperon puzzle", we consider that the repulsive MBE works also in hyperonic channels. As a specific model for MBE, the multi-pomeron exchange repulsion (MPP) is added to the two-body interaction together with the phenomenological three-body attraction (TBA).

We adjust MBE so as to reproduce the observed data of B_Λ. Then, it is evident that the strength of MBE depends on the two-body interaction model. Even among various versions of the Nijmegen interaction models (ESC08a/b, ESC12, ESC14, ESC04a, NSC97e/f), there are considerable differences with each other. Especially, important is the difference among the P-state contributions. In the cases of ESC14 and ESC08a/b, the P-state contributions are almost vanishing, where the mass dependence of B_Λ can be reproduced well by adding MBE with the strong MPP repulsion assuring the stiff EoS of hyperon-mixed neutron-star matter. In the cases of ESC12 and NSC97e/f, the P-state contributions are substantially repulsive and helpful to reproduce the mass dependence of B_Λ: There is no room to introduce

TABLE X: Calculated values of B_Λ [MeV] for the ground and p-states of ${}^{40}_{\Lambda}$K and ${}^{48}_{\Lambda}$K with ESC12 + MBE and ESC14 + MBE. In the p-states k_F calculated by ADA is tuned as $k'_F = (1+\alpha)k_F$ using $\alpha = 0.010$ and 0.020 ($\alpha = 0.015$ and 0.025) for ESC12 + MBE (ESC14 + MBE). $\langle\rho\rangle$ [fm^{-3}], k'_F [fm^{-1}] and spin-parity J^π are also listed.

	Ground states					p-states				
	$\langle\rho\rangle$	α	k'_F	J^π	$-B_\Lambda$	$\langle\rho\rangle$	α	k'_F	J^π	$-B_\Lambda$
ESC14 + MBE										
${}^{40}_{\Lambda}$K	0.136	0.000	1.263	1^+	−19.4	0.109	0.015	1.191	2^-	−10.4
						0.109	0.025	1.202	2^-	−10.1
${}^{48}_{\Lambda}$K	0.141	0.000	1.278	1^+	−20.2	0.117	0.015	1.219	1^-	−11.6
						0.117	0.025	1.231	1^-	−11.3
ESC12 + MBE										
${}^{40}_{\Lambda}$K	0.136	0.000	1.263	1^+	−19.4	0.109	0.010	1.185	2^-	−10.2
						0.109	0.020	1.196	2^-	−9.9
${}^{48}_{\Lambda}$K	0.141	0.000	1.278	1^+	−20.2	0.117	0.010	1.213	1^-	−11.5
						0.117	0.020	1.225	1^-	−11.2

the strong MPP repulsion consistently with the experimental data. In the case of ESC04a, the P-state contribution is strongly attractive, and it is difficult to reproduce the mass dependence of B_Λ by adding the present form of MBE.

The B_Λ values of hypernuclei with $9 \le A \le 59$ are analyzed in the framework of HyperAMD with use of the ΛN G-matrix interactions derived from ESC14 and ESC12. In both cases, the calculated values of B_Λ reproduce the experimental data within a few hundred keV, when MBE is taken into account. The values of B_Λ and E_x in p-states also can be reproduced well by the HyperAMD, when the ADA is modified so as to make input values of k_F slightly larger for weakly-bound Λ states. Though the results for ESC14 and ESC12 are quite similar to each other, the strength of MPP repulsion included in MBE for ESC12 is far weaker than that for ESC14: The former (ESC14) is strong enough to give rise to the stiff EoS of hyperon-mixed neutron star-matter, but the latter (ESC12) is not.

In the present, it is difficult to prove the existence of MBE including strong repulsion on the basis of the experimental data of B_Λ, because the two-body interaction model is not finely determined. However, we can say at least as follows: The possible existence of the strong hyperonic repulsions suggested by the stiff EoS of neutron stars is compatible with ΛN interaction models giving almost vanishing contributions of P-state interactions.

The Fortran codes ESC08c2012.f (ESC12), ESC08c2014.f (ESC14), and HNPOTESC16.f (ESC16) can be found on the permanent open-access website NN-Online: *http://nn-online.org*.

[1] P.M.M.Maessen, T.A.Rijken, and J.J.deSwart, Phys. Rev. C**40**, 2226(1989).
[2] Th.A. Rijken, V.G.J. Stoks, and Y. Yamamoto, Phys. Rev. C**59**, 21(1999).
[3] Th.A.Rijken and Y.Yamamoto, Phys. Rev. C**73**, 044008(2006).
[4] Th.A. Rijken, M.M. Nagels, and Y. Yamamoto, Prog. Theor. Phys. Suppl. **185**, 14 (2010).
[5] B. Holzenkamp, K. Holinde, and J. Speth, Nucl. Phys. A**500**, 485 (1989).
[6] A. Reuber, K. Holinde, and J. Speth, Nucl. Phys. A**570**, 543 (1994).
[7] Y.Fujiwara, Y.Suzuki and C.Nakamoto, Prog. Part. Nucl. Phys. **58**, 439(2007).
[8] P.B. Demorest, T. Pennucci, S.M. Ransom, M.S.E. Roberts, and J.W. Hessels, Nature (London) **467**, 1081 (2010).
[9] J. Antoniadis *et al.*, Science **340**, 6131 (2013).
[10] M. Baldo, G.F. Burgio, and H.-J. Schulze, Phys. Rev. C**61**, 055801(2000).
[11] I. Vidana, A. Polls, A. Ramos, L. Engvik, and M. Hjorth-Jensen, Phys. Rev. C**62**, 035801(2000).
[12] S. Nishizaki, Y. Yamamoto, and T. Takatsuka, Prog. Theor. Phys. **105**, 607 (2001); **108**, 703 (2002).
[13] Y.Yamamoto, T.Furumoto, N.Yasutake and Th.A.Rijken, Phys. Rev. C**90**, 045805(2014).
[14] D. Lonardoni and F. Pederiva, Phys. Rev. C**89**, 014314(2014).
[15] Y.Yamamoto, T.Furumoto, N.Yasutake and Th.A.Rijken, Phys. Rev. C**88**, 022801(2013).
[16] D. Lonardoni, A. Lovato, S. Gandolfi, and F. Pederiva, Phys. Rev. Lett. **114**, 092301(2015).
[17] M. Isaka, Y. Yamamoto and Th.A. Rijken, Phys. Rev. C, accepted: arXiv:1609.06009 (2016).
[18] M.M.Nagels, T.A.Rijken and J.J.deSwart, Phys. Rev. D**15** (1977), 2547; D**20**, 1633(1979).
[19] Th.A. Rijken, M.M. Nagels, and Y. Yamamoto, in *Proceedings of the International Workshop on Strangeness Nuclear Physics*, Neyagawa 2012, Genshikaku Kenkyu **57**, Suppl.3, 6 (2013).
[20] M.M. Nagels, Th.A. Rijken, and Y. Yamamoto, arXiv:1408.4825 (2014).
[21] M.M. Nagels, Th.A. Rijken, and Y. Yamamoto, arXiv:1501.06636 (2015).

[22] M.M. Nagels, Th.A. Rijken, and Y. Yamamoto, arXiv:1504.02634 (2015).
[23] M.M. Nagels, Th.A. Rijken, and Y. Yamamoto, Phys. Rev. C, submitted.
[24] Y.Yamamoto, T.Motoba, and Th.A. Rijken, Prog. Theor. Phys. Suppl. **185**, 72(2010).
[25] O. Hashimoto and H. Tamura, Prog. Part. and Nucl. Phys. **57**, 564(2006).
[26] R. Bertini *et al.*, Phys.Lett. B**83**, 306(1979).
[27] D.H. Davis, Nucl. Phys. A**547**, 369(1992).
[28] S. Ajimura *et al.*, Nucl. Phys. A**639**, 93c(1998).
[29] H. Tamura *et*. *a*l., Nucl. Phys. A**754**, 58c(2005).
[30] R. E. Chrien *et al.*, Phys. Rev.C**41**, 1062(1990).
[31] D. Ziemińska, Nucl. Phys. A**242**, 461(1975).
[32] D. Kielczewska, *et al.*, Nucl. Phys. A**238**, 437(1975).
[33] D. Ziemińska, R.H. Dalitz, Nucl. Phys. A**238**, 453(1975).
[34] D. Kielczewska, D. Ziemińska, R.H. Dalitz, Nucl. Phys. A**333**, 367(1980).
[35] H. Tamura *et al.*, Nucl. Phys. A**835**, 3(2010).
[36] M. Ukai *et al.*, Phys. Rev. Lett. **93**, 232501(2004).
[37] D.H. Davis, Nucl. Phys. A**754**, 3c(2005).
[38] M. Jurič *et al.*, Nucl. Phys. B**52**, 1(1973).
[39] P.H. Pile *a*l., Phys. Rev. Lett. **66**, 2585(1991).
[40] H. Hotchi *a*l., Phys. Rev. C**64**, 044302(2001).
[41] L. Tang, *e*t. *a*l., Phys. Rev. C**90**, 034320(2014).
[42] T. Gogami *et al.*, Phys. Rev. C**93**, 034314(2016).
[43] J. Decharge and D. Gogny, Phys. Rev. C**21**, 1568(1980) .
[44] J.F. Berger, M. Girod and D. Gogny, Comp. Phys. Comm.**63**, 365(1991).
[45] G.Audi, *et al.*, Chinese Physics C**36**, 1287(2012).
[46] S. Ajimura, *et al.*, Phys. Rev. Lett.**86**, 4255(2001).
[47] H. Kohri, *et al.*, Phys. Rev. C**65**, 034607(2002).
[48] T. Hasegawa, *et al.*, Phys. Rev. C**53**, 1210(1996).
[49] F. Garibaldi, *et al.* (JLab Hypernuclear Collaboration), proposal to JLab PAC44(2016).
[50] F. Pederiva, *et al.*, arXiv:1506.04042v1.